DOI:
10.1109/TFUZZ.2021.3090923

Document Version
Peer reviewed version

Aperiodic Sampled-Data Takagi-Sugeno Fuzzy Extended State Observer for A Class of Uncertain Nonlinear Systems with External Disturbance and Unmodeled Dynamics

Zhichen Li, Hao Zhang, Huaicheng Yan, Hak-Keung Lam, and Congzhi Huang

***Abstract*—In this paper, the problem of sampled-data extended state observer (ESO) design is considered for a class of uncertain nonlinear systems. Firstly, based on the fuzzy modeling approach with reasonable fuzzy rules and sets, the nonlinear functions of the ESO are suitably approximated by several local linear models weighted by membership functions. Then, in order to estimate the total disturbance including external disturbance and unmodeled dynamics, a novel methodology of Takagi-Sugeno fuzzy extended state observer (TSFESO) is developed for the first time. By virtue of fuzzy membership functions, the estimating action is implemented in nonlinear pattern, while taking advantages of T-S fuzzy formulation, the observer gains can be calculated in linear manner. As a result, the nonlinear estimating efficiency and linear numerical tractability are integrated in a unified framework. Secondly, for the aperiodic sampling case, the exponential convergence criterion for the TSFESO is presented by constructing a sampling- and time-dependent Lyapunov function, in which the information on output error and sampling action is taken into full consideration for desirable feasibility. Moreover, the observer design approach is also put forward. Finally, the superiorities and effectiveness of the proposed approaches are demonstrated by an illustrative numerical example. For the TSFESO, the dilemma choice between nonlinear operation efficiency and linear proof convenience is addressed. In addition, a generalized ESO formation is provided to be compatible of non-additive constraint factors, which cannot be categorized into total disturbance, and thus the application scope of ESO is further broadened.**

***Index Terms*—Uncertain nonlinear systems, Takagi-Sugeno fuzzy extended state observer (TSFESO), aperiodic sampled-data, sampling- and time-dependent Lyapunov function (STDLF).**

I. Introduction

In real-world applications, almost all of the practical systems and industrial processes are of intrinsically nonlinear property [1-3], such as mass-spring-damping system [4], one-link robotic manipulator [5], and stirred tank reactor [6]. Nonlinearity is naturally apt to be realistic for dynamic description [7], while inevitably exerts a formidable obstacle on analysis and synthesis [8]. Thanks to the preferable structure comprising a family of local linear models in various variable subspaces connected by fuzzy membership functions, the Takagi-Sugeno (T-S) fuzzy model has shown favorable performance in approximating any smooth nonlinearity in a compact set to any degree of accuracy [9, 10]. Accordingly, the past few years have witnessed tremendous prosperity on performance analysis [11, 12], control synthesis [13-15], and filter/observer design [16, 17] for T-S fuzzy systems.

In modern engineering field, a wide variety of uncertainties in the forms of external disturbance and unmodeled dynamics unavoidably cause performance deterioration, or even instability [7]. It is noted that the T-S fuzzy model is qualified to express the exactly known nonlinear systems. Consequently, the uncertainty considered in such context is generally confined to the norm-bounded variable parameters multiplied by system matrices [12, 14, 17]. Furthermore, from the perspective of disturbance suppression, the ultimate purpose of this line is to attenuate negative influence to satisfy prescribed performance levels, such as $(\mathcal{Q},\mathcal{S},\mathcal{R})$-dissipative [3], $\mathcal{L}_2$-$\mathcal{L}_\infty$ [10], and $\mathcal{H}_\infty$ [12] indexes, which is passively tolerant in presence of disturbance, but lacks active mechanism from the sight of disturbance rejection and compensation.

As a powerful control strategy in dealing with unmeasured uncertainty, active disturbance rejection control (ADRC) has been initially proposed by Han [18]. The essential philosophy for ADRC is to extract external disturbance and unmodeled dynamics as the total disturbance represented by an extended state, and then estimate it through an extended state observer (ESO), and finally compensate for it via control action in real time [19-21]. By right of distinct attribute requiring very little information on plant dynamics, as a centerpiece of ADRC, the ESO has found a surge of successful applications in gasoline engine [22], mobile robot [23], and induction machine [24]. According to specific formulations for observation functions, the ESO can be classified into two typical categories: nonlinear ESO (NESO) and linear ESO (LESO).

By virtue of flexible nonlinear structure, NESO is endowed with excellent estimation efficiency [19, 24]. Unfortunately, suffering from the sophisticated framework, rigorous stability analysis is no mean feat for NESO. In order to avoid multi-gain adjustment, by introducing a tunable parameter ε, a special case of NESO is developed in [25] with strict convergence proof. Since then, diversified versions of ε-dependent NESO

This work is supported by the National Natural Science Foundation of China (61673178, 61773289).

Z. Li and H. Yan are with School of Information Science and Engineering, East China University of Science and Technology, Shanghai 200237, China (e-mail: zcli@ecust.edu.cn; hcyan@ecust.edu.cn).
H. Zhang is with Department of Control Science and Engineering, Tongji University, Shanghai 200092, China (e-mail: zhang_hao@tongji.edu.cn).
H. K. Lam is with the Department of Engineering, King's College London, London, WC2R 2LS, U.K. (e-mail: hak-keung.lam@kcl.ac.uk).
C. Huang is with the School of Control and Computer Engineering, North China Electric Power University, Beijing 102206, China (e-mail: hcz190@ncepu.edu.cn).

are extended to some actual situations, such as actuator saturation [26], mismatched uncertainties [27], and event-triggered mechanism [28]. However, numerous assumptions are made for derivation, and the proof processes are extremely complicated. For instance, in order to accommodate NESO, a Lyapunov function-related event-triggered mechanism (ETM) is presented in [28], and additional proof is implemented to guarantee nonzero dwell-time interval. Some improved adaptive and dynamic ETMs [3, 16] and sampled-data-based ETM [13] intrinsically free of Zeno phenomenon are inapplicable for NESO design. As a result, further extension of NESO is especially restricted for some considerations incompatible of total disturbance, such as parameter switching [10], multi-density quantization [16], and incomplete measurement [17]. For theoretical accessibility, LESO is proposed as an alternative solution to facilitate parameter tuning [29]. Whereas, as indicated in [18], the simplification of LESO is achieved at sacrifice of loss of design flexibility. In addition, observer gains assignment resorts to the bandwidth-parameterized technique based on pole-placement method [30]. Referring to the aperiodic sampling interval and time-varying delay, the estimation error dynamics is an infinite dimensional system, and the corresponding characteristic equation can be exactly described by transcendental equation, which presents dramatic difficulty in determining eigenvalues. In response to above discussions, a crucial issue is raised: how to exploit a desirable ESO of sufficient operational flexibility, rigorous mathematical vindicability, and convenient numerical solvability, which is one of the primary motivations behind this paper.

With rapid advancement of digital network communication technology, the sampled-data systems [2, 5, 13] have experienced a meteoric rise specific to a growing demand for less transmission burden. In network environment, a sampled-data ESO (SDESO) is presented for disturbed systems, while only constant sampling case is taken into account [31]. In view of communication constraints, the sampling operation practically tends to be aperiodic. In [32], the sampled instant is recognized as the event-triggered one, and thus whether to transmit data is determined by the prescribed ETM, in which maximum allowable sampling interval cannot be computed. Considering actuator saturation, a SDESO is proposed for pneumatic muscle actuator [33]. It is noticeable that the sampling interval is of complex coupling relation with Lipschitz constant for nonlinear observer function and constraint condition of Lyapunov function. As a consequence, the upper bound for sampling interval can be obtained, only if a variety of parameters are well selected. Thus, in aperiodic sampling case, how to give a preferable SDESO design approach suitable for simultaneous acquisition of stable sampling interval and observer gains is a challenging task, which is another motivation of this paper.

Inspired by aforementioned issues, the primary purpose of this paper is to find an effective ESO strategy for a class of uncertain nonlinear systems. The main contributions of the proposed approaches can be summarized as follows:

(i) By setting proper premise variables and fuzzy sets, a novel T-S fuzzy ESO (TSFESO) is developed to estimate both of the system states and total disturbance. In the local subsystems, the observer gains are presented in linear form, while by virtue of membership functions, the TSFESO works in nonlinear pattern. The preknowledge of the uncertainty is unnecessary for observer design, and the concerned total disturbance can be given in any form with only bound on the derivative.

(ii) In regard to the TSFESO, the convergence analysis of the estimation error dynamics subject to aperiodic sampling is presented in sense of exponential boundedness. By constructing a sampling- and time-dependent Lyapunov function, the information on sampling action and output error is sufficiently reflected. Moreover, the relationships among fuzzy membership-related parameters characterizing NESO, variable sampling interval, decay rate, decay coefficient, and estimated bound are established quantitatively, and further consolidated by matrix variables.

(iii) The TSFESO design approach is proposed in terms of linear matrix inequalities (LMIs) independent of the bandwidth techniques. On the one hand, a complete TSFESO scheme is developed, which can be readily applied for states and uncertainty estimation. On the other hand, some communication- or network-induced phenomena difficult to analyze in nonlinear context are compatible in this framework. By feat of T-S fuzzy approach, the diversiform linear theory tools including advanced Lyapunov function and improved integral inequalities, are integrated into flexible NESO architecture.

The remainder of this paper is briefly outlined as follows. Section II presents the problem formulation and preliminaries. In Section III, sampled-data TSFESO is constructed. Section IV gives the convergence criterion and design approach for TSFESO. In Section V, a numerical example is provided to demonstrate the effectiveness of the proposed methods. The conclusion is drawn in Section VI.

Notations. $\mathbb{R}^n$ is n-dimensional Euclidean space; The superscripts T and -1 stand for transpose and inverse of matrix, respectively; $\mathrm{diag}\{\cdot\}$ denotes a block diagonal matrix; $\mathscr{S} > 0$ (< 0) means $\mathscr{S}$ being a symmetric positive (negative) definite matrix; $\mathbf{0}$ and $\mathbf{I}$ are zero and identity matrices of appropriate dimensions, respectively; $\star$ represents a term induced by symmetry; $\mathrm{Sym}\{\mathscr{S}\} = \mathscr{S} + \mathscr{S}^\top$; col$\{\cdot\}$ is a column vector; $\rho_{\min}(\mathscr{S})$ and $\rho_{\max}(\mathscr{S})$ refer to the minimum and maximum eigenvalues of matrix $\mathscr{S}$, respectively.

II. Problem Formulation and Preliminaries

Consider a class of n-dimensional single-input-single-output nonlinear continuous-time systems with uncertainty:

$$\begin{cases} x^{(n)}(t) = f(t, x(t), \dot{x}(t), \cdots, x^{(n-1)}(t)) + w(t) + u(t) \\ y(t) = x(t), \end{cases} \tag{1}$$

where $y \in C(\mathbb{R}, \mathbb{R})$ stands for the measurement output; $u \in C(\mathbb{R}, \mathbb{R})$ denotes the control input; $w \in C(\mathbb{R}, \mathbb{R})$ is the uncertain external disturbance; $f \in C(\mathbb{R}^n, \mathbb{R})$ represents the unmodeled system dynamics viewed as internal disturbance.

Defining $x_1(t) = x(t)$, $x_i(t) = x^{(i-1)}(t)$ $(i = 2, \cdots, n)$, $x_{n+1}(t) = f + w$, and $\dot{x}_{n+1}(t) = \phi(t)$, the nonlinear system

(1) can be rewritten as the following integrator cascade form

$$\begin{cases}\dot{x}_1(t)=x_2(t)\\ \vdots\\ \dot{x}_{n-1}(t)=x_n(t)\\ \dot{x}_n(t)=x_{n+1}(t)+u(t)\\ \dot{x}_{n+1}(t)=\phi(t)\\ y(t)=x_1(t).\end{cases} \tag{2}$$

Then, the following assumption is made for (2).

Assumption (H1). 1) The function f and the disturbance w are unknown in the sense that neither their explicit expressions nor the efficient estimations are available for ESO design.

2) For a scalar $\sigma \geq 0$, f and w are differentiable and satisfy

$$|\phi| = |\dot{f}+\dot{w}| \leq \sigma. \tag{3}$$

Accordingly, in [18], a NESO can be designed as follows:

$$\begin{cases}\dot{\hat{x}}_1(t)=\hat{x}_2(t)-\eta_1\vartheta_1(z_1(t))\\ \vdots\\ \dot{\hat{x}}_{n-1}(t)=\hat{x}_n(t)-\eta_{n-1}\vartheta_{n-1}(z_1(t))\\ \dot{\hat{x}}_n(t)=\hat{x}_{n+1}(t)-\eta_n\vartheta_n(z_1(t))+u(t)\\ \dot{\hat{x}}_{n+1}(t)=-\eta_{n+1}\vartheta_{n+1}(z_1(t)),\end{cases} \tag{4}$$

where $[\hat{x}_1(t),\cdots,\hat{x}_{n+1}(t)]^\top$ are the states of NESO, $z_1(t)=\hat{x}_1(t)-x_1(t)$, η_i $(i=1,\cdots,n+1)$ are the observer gains to be determined, and $\vartheta_i(\cdot)$ are a set of nonlinear functions.

The primary principle of ESO is to treat both of internal disturbance f and external disturbance w as a total disturbance, and express it as an extended state of system x_{n+1}, and thus for properly chosen functions $\vartheta_i \in C(\mathbb{R},\mathbb{R})$, the system states x_p $(p=1,2,\cdots,n)$ and the total disturbance $f+w$ can be approximated by $\hat{x}_i$ via regulating η_i $(i=1,2,\cdots,n+1)$.

Remark 1: In the original NESO (4), it is found that $n+1$-parameters are introduced, bringing barriers for theory analysis and parameter tuning. In a list of mainstream literatures [25-28], setting $\eta_i=-\varepsilon^{n-i}$ and $z_1(t)=[y(t)-\hat{x}_1(t)]/\varepsilon^n$, a nonlinear generalized ESO is developed to form one-parameter-related issue, and thus the ε-dependent convergence result is established. However, the nonlinear structure complicates the deriving procedure without good extensibility, and a certain degree of design flexibility is still lost, since the observer gains are regulated in a fixed ratio as $\{\varepsilon^{n-1}:\varepsilon^{n-2}:\cdots:\varepsilon^{-1}\}$.

The main concern of this paper is to develop a novel type of sampled-data ESO design approach to exploit preferable efficiency of NESO and desirable tractability of LESO.

III. The Franmework for Takagi-Sugeno Fuzzy Extended State Observer (TSFESO)

In this section, novel structure of T-S fuzzy ESO (TSFESO) is proposed, in which the estimating fashion is presented in nonlinear manner, while the observer gains are given in linear form. Thus, the merits for LESO and NESO are integrated in a unified framework.

A. Takagi-Sugeno Fuzzy Extended State Observer (TSFESO)

The nonlinear functions $\vartheta_i(\cdot)$ are crucial for characterizing the ESO in a nonlinear fashion. Without loss of generality, suppose that $z_1(t)$ varies within a range of $[-\iota,\iota]$ with $\iota>0$. $\vartheta_i(\cdot)$ are assumed to satisfy the following conditions:

Assumption (H2). 1) For any scalars $\theta_1,\theta_2 \in [-\iota,\iota]$, each nonlinear function $\vartheta_i(\cdot):\mathbb{R}\to\mathbb{R}$ is continuous with

$$\vartheta_i(0)=0, \quad \frac{\vartheta_i(\theta_1)-\vartheta_i(\theta_2)}{\theta_1-\theta_2} \geq 0 \quad \theta_1\neq\theta_2. \tag{5}$$

2) For any $\theta\in[-\iota,\iota]$, there exist two linear continuously differentiable functions $\mathscr{U}_{i1}(\cdot)$ and $\mathscr{U}_{i2}(\cdot):\mathbb{R}\to\mathbb{R}$ such that

$$\mathscr{U}_{i1}(0)=\mathscr{U}_{i2}(0)=0, \tag{6}$$

$$|\mathscr{U}_{i1}(\theta)| \leq |\vartheta_i(\theta)| \leq |\mathscr{U}_{i2}(\theta)|, \tag{7}$$

$$\mathscr{U}_{i1}(\iota)=\vartheta_i(\iota), \quad \mathscr{U}_{i1}(-\iota)=\vartheta_i(-\iota). \tag{8}$$

Remark 2: A series of conditions are placed on the nonlinear functions. In practice, (5)-(8) hardly impose extra restriction on $\vartheta_i(\cdot)$, since the *Assumption* (H2) is readily accessible for almost all of the nonlinear functions for formulating NESO in the existing literatures.

- In the seminal work [18], the fal$(\cdot)$ function is proposed as the nonlinear functions of NESO in the following form:

$$\vartheta_i(\theta)=\mathrm{fal}(\theta,a,\delta)=\begin{cases}|\theta|^a\mathrm{sign}(\theta) & |\theta|\geq\delta\\ \dfrac{1}{\delta^{1-a}}\theta & |\theta|<\delta\end{cases} \tag{9}$$

with $\delta>0$ and $0<a\leq1$ being constants shaping $\vartheta_i(\cdot)$.

On the one hand, it is obvious that $\vartheta_i(0)=\mathrm{fal}(0,a,\delta)=0$. For $\theta\in(-\infty,+\infty)$, $\mathrm{fal}(\theta,a,\delta)$ is a piecewise continuous function. Moreover, it is noticed that $h_1(\theta)=|\theta|^a\mathrm{sign}(\theta)$ and $h_2(\theta)=k\theta$ $(k>0)$ are monotonically increasing, and thus (5) is satisfied. On the other hand, the differentiating calculation yields

$$\left|\mathrm{fal}'(\theta,a,\delta)\right|=\begin{cases}a|\theta|^{a-1} & |\theta|\geq\delta\\ \dfrac{1}{\delta^{1-a}} & |\theta|<\delta.\end{cases} \tag{10}$$

Given $a\in(0,1]$, for any $\theta\in[-\iota,\iota]$ with $\iota\geq\delta$, it always holds that $|\mathrm{fal}(\iota,a,\delta)\theta/\iota| \leq |\mathrm{fal}(\theta,a,\delta)| \leq \left|\mathrm{fal}'(0,a,\delta)\theta\right|$. Therefore, the linear functions $\mathscr{U}_{i1}(\cdot)$ and $\mathscr{U}_{i2}(\cdot)$ can be chosen as $\mathscr{U}_{i1}(\theta)=\iota^{a-1}\theta$ and $\mathscr{U}_{i2}(\theta)=\delta^{a-1}\theta$ to guarantee the truth of (6)-(8).

- In a number of recent contributions [26-28, 32, 33], for a 2-dimensional nonlinear system, the ESO is specified by

$$\vartheta_1(\theta)=r_1\theta+\psi(\theta), \quad \vartheta_2(\theta)=r_2\theta, \quad \vartheta_3(\theta)=r_3\theta \tag{11}$$

with $\psi(\cdot):\mathbb{R}\to\mathbb{R}$ being nonlinear function given as

$$\psi(\theta)=\begin{cases}b\mathrm{sign}(\theta) & |\theta|>0.5\pi\\ b\sin(\theta) & |\theta|\leq0.5\pi,\end{cases} \tag{12}$$

where $r_i>0$ $(i=1,2,3)$ and $0<b<1$ are constants.

Firstly, it is easy to find that $\vartheta_i(0)=0$. In addition, owning to the nondecreasing property for $\vartheta_i(\cdot)$, (5) holds. Secondly, $|\vartheta_1'(\cdot)|$ reaches the maximum value at $\theta=0$, and then for $\iota>0.5\pi$, it gives that $|b\theta/\iota+r_1\theta| \leq |\vartheta_1(\theta)| \leq |b\cos(0)\theta+r_1\theta|$. Thus, selection of $\mathscr{U}_{11}(\theta)=b\theta/\iota+r_1\theta$ and $\mathscr{U}_{12}(\theta)=(b+r_1)\theta$

such that (6)-(8) are ensured. Thirdly, in view of the linearity of $\vartheta_2(\cdot)$ and $\vartheta_3(\cdot)$, one can directly set $\mathscr{U}_{21}(\theta) = \mathscr{U}_{22}(\theta) = r_2\theta$ and $\mathscr{U}_{31}(\theta) = \mathscr{U}_{32}(\theta) = r_3\theta$. As a result, the *Assumption* (H2) is satisfied for $\vartheta_i(\cdot)$ in (11).

In order to construct the T-S fuzzy model for NESO, select $\xi_i(z_1) = \vartheta_i(z_1(t))$ as the premise variable for exploiting more nonlinear information. For the tradeoff between approximation accuracy and model simplicity, define the following two fuzzy sets for $\xi_i(z_1)$:

$\mathscr{L}_{i1}$: $\xi_i(z_1)$ is about $\mathscr{U}_{i1}(\cdot)$, at which $\xi_i(\iota) = \mathscr{U}_{i1}(\iota)$ and $\xi_i(-\iota) = \mathscr{U}_{i1}(-\iota)$;

$\mathscr{L}_{i2}$: $\xi_i(z_1)$ is about $\mathscr{U}_{i2}(\cdot)$, at which $\xi_i(0) = \mathscr{U}_{i2}(0)$.

Then, denote the membership value of $\xi_i(z_1)$ in $\mathscr{L}_{iq}$ as $\mathscr{L}_{iq}(\xi_i(z_1))$ $(q = 1, 2)$. Based on the *Assumption* (H2), each nonlinear function $\vartheta_i(z_1(t))$ can be expressed as the convex combination form by the sector nonlinearity fuzzy modeling method:

$$\begin{cases} \vartheta_i(z_1(t)) = \big[\mathscr{L}_{i1}(\xi_i(z_1))\mathscr{U}'_{i1}(\cdot) + \mathscr{L}_{i2}(\xi_i(z_1))\mathscr{U}'_{i2}(\cdot)\big] z_1(t) \\ 1 = \mathscr{L}_{i1}(\xi_i(z_1)) + \mathscr{L}_{i2}(\xi_i(z_1)), \end{cases} \tag{13}$$

where $\mathscr{U}'_{iq}(\cdot)(q = 1, 2)$ are the slopes for $\mathscr{U}_{iq}(\cdot)$.

Computing the solution of (13) gives

$$\begin{cases} \mathscr{L}_{i1}(\xi_i(z_1)) = \dfrac{\mathscr{U}'_{i2}(\cdot)z_1(t) - \vartheta_i(z_1(t))}{\Big[\mathscr{U}'_{i2}(\cdot) - \mathscr{U}'_{i1}(\cdot)\Big] z_1(t)} \\ \mathscr{L}_{i2}(\xi_i(z_1)) = \dfrac{\vartheta_i(z_1(t)) - \mathscr{U}'_{i1}(\cdot)z_1(t)}{\Big[\mathscr{U}'_{i2}(\cdot) - \mathscr{U}'_{i1}(\cdot)\Big] z_1(t)}. \end{cases} \tag{14}$$

Then, the local TSFESO can be presented as

Fuzzy Rule $\mathscr{S}_j$: **IF** $\xi_1(z_1)$ is $\mathscr{L}_{1q}(\xi_1(z_1))$ and $\cdots$ and $\xi_{n+1}(z_1)$ is $\mathscr{L}_{(n+1)q}(\xi_{n+1}(z_1))$, **THEN**

$$\begin{cases} \dot{\hat{x}}_1(t) = \hat{x}_2(t) - \eta_{1j}c_{1j}z_1(t) \\ \vdots \\ \dot{\hat{x}}_{n-1}(t) = \hat{x}_n(t) - \eta_{(n-1)j}c_{(n-1)j}z_1(t) \\ \dot{\hat{x}}_n(t) = \hat{x}_{n+1}(t) - \eta_{nj}c_{nj}z_1(t) + u(t) \\ \dot{\hat{x}}_{n+1}(t) = -\eta_{(n+1)j}c_{(n+1)j}z_1(t), \end{cases} \tag{15}$$

where $j = 1, \cdots, \kappa$ with $\kappa = 2^{(n+1)}$, and the nonlinear functions $\vartheta_i(z_1(t))$ in (4) are replaced by $c_{ij}z_1(t)$ with c_{ij} taking value from $\big\{\mathscr{U}'_{i1}(\cdot), \mathscr{U}'_{i2}(\cdot)\big\}$.

Therefore, the global dynamic of the TSFESO is inferred as a compact presentation:

$$\dot{\hat{x}}(t) = \sum_{j=1}^{\kappa} \mathscr{D}_j(\xi(z_1))\big[\mathcal{A}\hat{x}(t) + \mathcal{B}u(t) + \mathcal{C}_j\mathcal{G}_j z_1(t)\big], \tag{16}$$

where $\hat{x}(t) = [\hat{x}_1(t), \cdots, \hat{x}_{n+1}(t)]^\top$, $\mathscr{D}_j(\xi(z_1))$ are the normalized membership functions computed by

$$\mathscr{D}_j(\xi(z_1)) = \mathscr{L}_{1q}(\xi_1(z_1)) \times \cdots \times \mathscr{L}_{(n+1)q}(\xi_{n+1}(z_1)), \tag{17}$$

and the system matrices are listed as

$$\mathcal{A} = \begin{bmatrix} 0 & 1 & 0 & \cdots & 0 \\ 0 & 0 & 1 & \cdots & 0 \\ \vdots & \vdots & \vdots & \ddots & \vdots \\ 0 & 0 & 0 & \cdots & 1 \\ 0 & 0 & 0 & \cdots & 0 \end{bmatrix}, \mathcal{B} = \begin{bmatrix} 0 \\ 0 \\ \vdots \\ 1 \\ 0 \end{bmatrix}, \mathcal{G}_j = \begin{bmatrix} -\eta_{1j} \\ -\eta_{2j} \\ \vdots \\ -\eta_{nj} \\ -\eta_{(n+1)j} \end{bmatrix}$$

$$\mathcal{C}_j = \mathrm{diag}\Big\{c_{1j}, c_{2j}, \cdots, c_{nj}, c_{(n+1)j}\Big\}.$$

Remark 3: It is noted that the fuzzy-dependent observer gains $\mathcal{G}_j$ are introduced in the TSFESO to improve the design flexibility. When $\mathcal{G}_1 = \mathcal{G}_2 = \cdots = \mathcal{G}_\kappa$, (16) reduces to the fuzzy expression of NESO. Combining the *Assumption* (H1) with the features of membership values $\mathscr{L}_{ik}(\xi_i(z_1))$, the following properties for normalized membership functions $\mathscr{D}_j(\xi(z_1))$ are satisfied:

$$\mathscr{D}_j(\xi(z_1)) \geq 0, \quad \sum_{j=1}^{\kappa} \mathscr{D}_j(\xi(z_1)) = 1. \tag{18}$$

Remark 4: The appeal of T-S fuzzy model is to approximate nonlinear functions to any accuracy rating, in which the considered nonlinearity is required to be completely known. The innovation of ESO is to estimate the system uncertainty with little knowledge. In (16), a novel architecture referred to as Takagi-Sugeno fuzzy ESO (TSFESO) is proposed for the first time. The main characteristic for the TSFESO lies in that nonlinear state estimation pattern and linear local parameter existence are exploited, separately. As a consequence, the first attempt is devoted to integrate the effective utility for ESO into the systematic T-S fuzzy structure, the superiorities of which can be summarized as follows:

- *Linear Simplicity*: For the NESO, there exist a mass of predicaments in deriving the convergence criterion, especially in the case of aperiodic sampling actions. Based on the idea of sector nonlinearity, the fuzzy sets in regard to the properties of NESO are properly constructed. Blended by IF-THEN rules, the NESO is expressed as a family of local linear systems. In the developed TSFESO, the fundamental features of NESO are exploited by linear subsystems (15) coupled by membership functions. Thus, it is expected to implement the analysis by fruitful mathematical tools in linear system theory.
- *Nonlinear Efficiency*: For the LESO, the analytical simplicity is obtained at the expense of loss of nonlinear efficiency. In the proposed TSFESO, the nonlinear advantages are characterized by the membership functions with respect to original $\vartheta_i(z_1(t))$. Although the estimated error $z_1(t)$ is taken into consideration in linear manner, the TSFESO still operates in nonlinear fashion by means of a set of parameters $\mathcal{C}_j\mathcal{G}_j$ weighted by $\mathscr{D}_j(\xi(z_1))$. Thus, it is predicted that the flexible estimation capacity of nonlinear functions is allowed.

B. Sampled-Data TSFESO

For avoiding excessive data transmission, it is assumed that the measurement for observer input $z_1(t)$ is only sampled at the discrete sequence $\{t_k\}_{k\in\mathbb{N}}$, and remains constant during $[t_k, t_{k+1})$ by zero-order holder (ZOH) with $0 = t_0 < t_1 <$

$\cdots < t_k < \cdots < \lim_{k\to\infty} t_k = +\infty$. Considering a general situation with aperiodic sampling, the adjacent sampling interval is assumed to vary within the given range:

$$0 \leq h_m \leq h_k = t_{k+1} - t_k \leq h_M. \tag{19}$$

Injecting $z_1(t) = z_1(t_k)$ and $\xi_i(z_1) = \xi_i(z_1(t_k))$ into (15), for $t \in [t_k, t_{k+1})$, the TSFESO with sampled-data is proposed as

Fuzzy Rule $\mathscr{S}_j$: **IF** $\xi_1(z_1(t_k))$ is $\mathscr{L}_{1q}(\xi_1(z_1(t_k)))$ and $\cdots$ and $\xi_{n+1}(z_1(t_k))$ is $\mathscr{L}_{(n+1)q}(\xi_{n+1}(z_1(t_k)))$, **THEN**

$$\dot{\hat{x}}(t) = \mathcal{A}\hat{x}(t) + \mathcal{B}u(t) + \mathcal{C}_j\mathcal{G}_j z_1(t_k). \tag{20}$$

Similar to (16), $\forall t \in [t_k, t_{k+1})$, the overall sampled-data TSFESO is procured as

$$\dot{\hat{x}}(t) = \sum_{j=1}^{\kappa} \mathscr{D}_j(\xi(z_1(t_k)))\big[\mathcal{A}\hat{x}(t) + \mathcal{B}u(t) + \mathcal{C}_j\mathcal{G}_j z_1(t_k)\big]. \tag{21}$$

By setting $z_i(t) = \hat{x}_i(t) - x_i(t)$ $(i = 1, \cdots, n+1)$ and $z(t) = [z_1(t), \cdots, z_{n+1}(t)]^\top \in \mathbb{R}^{(n+1)}$, $\forall t \in [t_k, t_{k+1})$, the estimation error dynamics between sampled-data TSFESO (21) and nonlinear system (2) is governed by

$$\dot{z}(t) = \sum_{j=1}^{\kappa} \mathscr{D}_j(\xi(z_1(t_k)))\big[\mathcal{A}z(t) + \mathcal{C}_j\mathcal{G}_j\mathcal{E}z(t_k) + \mathcal{D}\phi(t)\big], \tag{22}$$

where $\mathcal{E} = [1, 0, \cdots, 0]$ and $\mathcal{D} = [0, 0, \cdots, 0, -1]^\top$.

C. Related Definition and Lemma

Definition 1: The estimation error system (22) is said to be exponentially ultimately bounded, if there exist scalars $\alpha > 0$, $\beta > 0$, and $\lambda > 0$ such that

$$\|z(t)\| \leq \alpha\|z(t_0)\|e^{-\lambda(t-t_0)} + \beta, \quad t \geq t_0, \tag{23}$$

where λ is the decay rate, and α is the decay coefficient.

Lemma 1 [34, 35]: For any constant matrix $\mathscr{Q} > 0$, and given scalars a and b with $a < b$, the following inequalities hold for all continuous function φ in $[a, b] \to \mathbb{R}^n$:

$$\int_a^b \varphi^\top(s)\mathscr{Q}\varphi(s)ds \geq \frac{1}{b-a}\Big(3\Theta_1^\top\mathscr{Q}\Theta_1 + \Theta_2^\top\mathscr{Q}\Theta_2\Big), \tag{24}$$

$$\int_a^b\int_\theta^b \varphi^\top(s)\mathscr{Q}\varphi(s)dsd\theta \geq \frac{2}{(b-a)^2}\Theta_3^\top\mathscr{Q}\Theta_3, \tag{25}$$

where

$$\Theta_1 = \frac{2}{b-a}\int_a^b\int_\theta^b \varphi(s)dsd\theta - \int_a^b \varphi(s)ds,$$
$$\Theta_2 = \int_a^b \varphi(s)ds,\ \Theta_3 = \int_a^b\int_\theta^b \varphi(s)dsd\theta.$$

Remark 5: The Wirtinger-based integral inequality is presented in (24), by which the feasible stability region will be enlarged by reducing the estimation gap of the Jensen one. To accommodate double integral Lyapunov function for reducing conservatism, Jensen double integral inequality (25) will be also utilized. In the next section, the effective linear analysis tools will be applied in ESO convergence criterion and design approach for the first time.

IV. Main Results

In this section, by establishing a novel Lyapunov function, an exponential convergence criterion is derived for the estimation error dynamics subject to non-periodic sampling. Moreover, the observer design approach is also presented by performing some appropriate transformations.

For narration simplicity, some notations are define as follows:

$$\upsilon(t) = \mathrm{col}\Big\{z(t), z(t_k), \int_{t_k}^t z(s)ds, \int_{t_k}^t\int_\theta^t \frac{z(s)}{t-t_k}dsd\theta, \dot{z}(t)\Big\},$$
$$\varrho = \mathrm{col}\Big\{e_1,\ e_2\Big\},\ \iota_1 = e_3,\ \iota_2 = 2e_4 - e_3,$$
$$\rho_1 = \mathrm{col}\Big\{e_1,\ e_2,\ e_3\Big\},\ \tau_1 = \mathrm{col}\Big\{e_1 - e_2,\ e_3\Big\},$$
$$\rho_2 = \mathrm{col}\Big\{e_5,\ \mathbf{0},\ e_1\Big\},\ \tau_2 = \mathrm{col}\Big\{e_5,\ e_1\Big\},$$
$$e_q = \big[\mathbf{0}_{(n+1)\times(q-1)(n+1)} \quad \mathbf{I}_{(n+1)\times(n+1)} \quad \mathbf{0}_{(n+1)\times(5-q)(n+1)}\big].$$

Theorem 1: Suppose that the *Assumptions* (H1) and (H2) hold. For the given scalars ψ_1, ψ_2, $h_M \geq h_m \geq 0$, $\lambda > 0$, and $\sigma > 0$, if there exist positive scalar γ, positive definite matrices $\mathcal{P}$, $\mathcal{Q}$, $\mathcal{Y} = [\mathcal{Y}_{ij}]_{2\times2}$, $\mathcal{X}$, symmetric matrices $\mathcal{T}$, $\mathcal{U} = [\mathcal{U}_{mn}]_{3\times3}$, $\mathcal{S} = [\mathcal{S}_{ij}]_{2\times2}$, and any matrices $\mathcal{H}_i$ $(i = 1, 2)$, $\mathcal{L}$, and $\mathcal{K}_j$ of appropriate dimensions such that the following inequalities are feasible at the vertices of $h_k \in [h_m, h_M]$ for $j = 1, \cdots, \kappa$:

$$\begin{bmatrix} h_M(\mathcal{U} + \mathscr{S}) + e^{-2\lambda h_M}\mathrm{diag}\Big\{\mathbf{0}, \mathbf{0}, \mathcal{Y}_{11}\Big\} & \begin{bmatrix}\mathbf{0}\\ \mathbf{0}\\ \mathcal{Y}_{12}\end{bmatrix} \\ \star & e^{2\lambda h_M}\mathcal{Y}_{22}\end{bmatrix} > 0, \tag{26}$$

$$\mathit{\Omega}_{1j}(h_k) = \mathit{\Lambda}_j + h_k\mathit{\Pi} < 0, \tag{27}$$

$$\mathit{\Omega}_{2j}(h_k) = h_k\begin{bmatrix} \mathit{\Gamma} + \frac{1}{h_k}\mathit{\Lambda}_j & \begin{bmatrix}\mathit{\Theta}_1^\top & \mathit{\Theta}_2^\top\end{bmatrix} \\ \star & -e^{2\lambda h_M}\begin{bmatrix}\mathcal{Y}_{11} & \mathbf{0}\\ \star & \frac{1}{3}\mathcal{Y}_{11}\end{bmatrix}\end{bmatrix} < 0, \tag{28}$$

the trajectory of sampled-data estimation error dynamics (22) is exponentially ultimately bounded with

$$\|z(t)\| \leq \sqrt{\frac{\rho_{\max}(\mathcal{P})}{\rho_{\min}(\mathcal{P})}}\|z(0)\|e^{-\lambda t} + \frac{\sigma}{\sqrt{2\lambda}}\sqrt{\frac{\gamma}{\rho_{\min}(\mathcal{P})}}, \tag{29}$$

and thus, the TSFESO is convergent to

$$\lim_{t\to+\infty}\|\hat{x}(t) - x(t)\| = \frac{\sigma}{\sqrt{2\lambda}}\sqrt{\frac{\gamma}{\rho_{\min}(\mathcal{P})}}. \tag{30}$$

Then, the corresponding observer gain matrices can be calculated as $\mathcal{G}_j = \mathcal{C}_j^{-1}\mathcal{L}^{-1}\mathcal{K}_j$, where

$$\begin{cases} \mathit{\Lambda}_j = \begin{bmatrix}\mathit{\Lambda}_{j11} & \mathit{\Lambda}_{12}\\ \star & -\gamma\mathbf{I}\end{bmatrix}, \quad \mathit{\Pi} = \begin{bmatrix}\mathit{\Pi}_{11} & \mathbf{0}\\ \star & \mathbf{0}\end{bmatrix} \\ \mathit{\Gamma} = \begin{bmatrix}\mathit{\Gamma}_{11} & \mathbf{0}\\ \star & \mathbf{0}\end{bmatrix}, \quad \mathit{\Theta}_i = \begin{bmatrix}\mathcal{H}_i & \mathbf{0}\end{bmatrix} \quad (i = 1, 2) \\ \mathit{\Lambda}_{j11} = 2\lambda e_1^\top\mathcal{P}e_1 - e_3^\top\mathcal{T}e_3 - \rho_1^\top\mathcal{U}\rho_1 + \mathrm{Sym}\Big\{e_1^\top\mathcal{P}e_5\Big\}\end{cases}$$

$$\begin{cases} \quad - e^{-2\lambda h_M}\mathrm{Sym}\Big\{e_3^\top \mathcal{Y}_{12}e_2\Big\} - 2e^{-2\lambda h_M}e_4^\top \mathcal{X}e_4 \\ \quad - \tau_1^\top \mathcal{S}\tau_1 - e^{-2\lambda h_M}\sum_{i=1}^{2}(2i-1)\mathrm{Sym}\Big\{\iota_i^\top \mathcal{H}_i\Big\} \\ \quad + \mathrm{Sym}\Big\{\Big(e_1^\top + \psi_1 e_2^\top + \psi_2 e_5^\top\Big) \\ \quad \times \Big(-\mathcal{L}e_5 + \mathcal{L}\mathcal{A}e_1 + \mathcal{K}_j\mathcal{E}e_2\Big)\Big\} \\ \Lambda_{12} = \Big[(\mathcal{L}\mathcal{D})^\top \quad \psi_1(\mathcal{L}\mathcal{D})^\top \quad \mathbf{0} \quad \mathbf{0} \quad \psi_2(\mathcal{L}\mathcal{D})^\top\Big]^\top \\ \Gamma_{11} = \Big(\frac{1}{2}\lambda h_M - 1\Big)e_2^\top \mathcal{Q}e_2 + \frac{1}{4}h_M e_1^\top \mathcal{X}e_1 \\ \quad - e^{-2\lambda h_M}e_2^\top \mathcal{Y}_{22}e_2 \\ \Pi_{11} = \Big(\frac{1}{2}\lambda h_M + 1\Big)e_2^\top \mathcal{Q}e_2 + \frac{1}{4}h_M e_1^\top \mathcal{X}e_1 + \varrho^\top \mathcal{Y}\varrho \\ \quad + 2\lambda e_3^\top \mathcal{T}e_3 + 2\lambda\Big(\rho_1^\top \mathcal{U}\rho_1 + \tau_1^\top \mathcal{S}\tau_1\Big) \\ \quad + \mathrm{Sym}\Big\{\rho_1^\top \mathcal{U}\rho_2 + \tau_1^\top \mathcal{S}\tau_2 + e_3^\top \mathcal{T}e_1\Big\} \end{cases}$$

with $\mathcal{H}_i = \begin{bmatrix} \mathcal{H}_{i1} & \mathcal{H}_{i2} & \mathcal{H}_{i3} & \mathcal{H}_{i4} & \mathcal{H}_{i5} \end{bmatrix}$, and

$$\mathcal{U} = \begin{bmatrix} \mathcal{U}_1 + \mathcal{U}_1^\top & -\mathcal{U}_1 - \mathcal{U}_2 & \mathcal{U}_3 \\ \star & \mathcal{U}_2 + \mathcal{U}_2^\top & \mathcal{U}_4 \\ \star & \star & \mathcal{U}_5 \end{bmatrix}$$

$$\mathscr{S} = \begin{bmatrix} \mathcal{S}_{11} & -\mathcal{S}_{11} & \mathcal{S}_{12} \\ \star & \mathcal{S}_{11} & -\mathcal{S}_{12} \\ \star & \star & \mathcal{T} + \mathcal{S}_{22} \end{bmatrix}.$$

Proof: Construct the sampling- and time-dependent Lyapunov function (STDLF) candidate as

$$V(t) = \sum_{m=1}^{6} V_m(t), \quad t \in [t_k,\ t_{k+1}), \tag{31}$$

where

$$\begin{aligned} V_1(t) =& z^\top(t)\mathcal{P}z(t) \\ V_2(t) =& (t_{k+1} - t)(t - t_k)z^\top(t_k)\mathcal{Q}z(t_k) \\ V_3(t) =& (t_{k+1} - t)\int_{t_k}^{t} z^\top(s)ds\mathcal{T}\int_{t_k}^{t} z(s)ds \\ V_4(t) =& (t_{k+1} - t)\Big[\eta^\top(t)\mathcal{U}\eta(t) + \gamma^\top(t)\mathcal{S}\gamma(t)\Big] \\ V_5(t) =& (t_{k+1} - t)\int_{t_k}^{t} e^{2\lambda(s-t)}\varpi^\top(s)\mathcal{Y}\varpi(s)ds \\ V_6(t) =& (t_{k+1} - t)\int_{t_k}^{t}\int_{\theta}^{t} e^{2\lambda(s-t)}z^\top(s)\mathcal{X}z(s)dsd\theta \end{aligned}$$

with $\gamma(t) = \mathrm{col}\Big\{z(t) - z(t_k),\ \int_{t_k}^{t} z(s)ds\Big\}$, $\varpi(t) = \mathrm{col}\Big\{z(t),\ z(t_k)\Big\}$, and $\eta(t) = \mathrm{col}\Big\{z(t),\ z(t_k),\ \int_{t_k}^{t} z(s)ds\Big\}$.

For $n = 2, \cdots, 6$, $\lim_{t\to t_k^-} V_n(t) = V_n(t_k) = 0$. Hence, it is deduced that $V(t)$ is continuous on $[0, \infty)$. In addition, it can be seen that $V_3(t)$ and $V_4(t)$ vanish at the sampling instants t_k and t_{k+1}, which implies that the looped function condition [36] is satisfied, and thus the Lyapunov matrices $\mathcal{T}$, $\mathcal{U}$, and $\mathcal{S}$ are unnecessary to be positive definite.

Define $\Psi = \mathcal{Y} - \mathrm{diag}\{\mathcal{Y}_{11} - \mathcal{Y}_{12}\mathcal{Y}_{22}^{-1}\mathcal{Y}_{12}^\top, \mathbf{0}\}$. After simple algebraic manipulation, Ψ can be written as

$$\Psi = \begin{bmatrix} \mathcal{Y}_{12}\mathcal{Y}_{22}^{-1}\mathcal{Y}_{12}^\top & \mathcal{Y}_{12} \\ \star & \mathcal{Y}_{22} \end{bmatrix}. \tag{32}$$

Based on the Schur complement with $\mathcal{Y}_{22} > 0$, it is obvious that $\Psi \geq 0$. Then, by the fact $\mathcal{Q} > 0$ and $\mathcal{X} > 0$, application of Jensen inequality leads to

$$\begin{aligned} &V(t) \geq V_1(t) + V_3(t) + V_4(t) + (t_{k+1} - t)\int_{t_k}^{t} e^{2\lambda(s-t)} \\ &\times \varpi^\top(s)\begin{bmatrix} \mathcal{Y}_{11} - \mathcal{Y}_{12}\mathcal{Y}_{22}^{-1}\mathcal{Y}_{12}^\top & \mathbf{0} \\ \star & \mathbf{0} \end{bmatrix}\varpi(s)ds \geq V_1(t) \\ &+ (t_{k+1} - t)\eta^\top(t)\Big(\mathcal{U} + \mathscr{S} + \frac{1}{h_M}e^{-2\lambda h_M}\mathscr{Y}\Big)\eta(t), \end{aligned} \tag{33}$$

where $\mathscr{Y} = \mathrm{diag}\{\mathbf{0},\ \mathbf{0},\ \mathcal{Y}_{11} - \mathcal{Y}_{12}\mathcal{Y}_{22}^{-1}\mathcal{Y}_{12}^\top\}$.

Consequently, one can deduce that

$$\begin{aligned} V(t) \geq& \eta^\top(t)\Big\{(t_{k+1} - t)\Big(\mathcal{U} + \mathscr{S} + \frac{1}{h_M}e^{-2\lambda h_M}\mathscr{Y}\Big) \\ &+ \mathrm{diag}\Big\{\mathcal{P},\ \mathbf{0},\ \mathbf{0}\Big\}\Big\}\eta(t). \end{aligned} \tag{34}$$

Implementing the Schur complement to (26) gives rise to $\mathcal{U} + \mathscr{S} + \frac{1}{h_M}e^{-2\lambda h_M}\mathscr{Y} > 0$. As a result, owning to $\mathcal{P} > 0$, it is concluded that $V(t) \geq z^\top(t)\mathcal{P}z(t)$, and thus

$$V(t) \geq \rho_{\min}(\mathcal{P})\|z(t)\|^2. \tag{35}$$

Summarizing the aforementioned analysis, the STDLF (31) is valid for construction of Lyapunov function.

Taking derivatives of individual Lyapunov functions of $V(t)$ along the trajectory of (22) yields

$$\begin{aligned} \dot{V}_1(t) + 2\lambda V_1(t) =& \mathrm{Sym}\Big\{z^\top(t)\mathcal{P}\dot{z}(t)\Big\} + 2\lambda z^\top(t)\mathcal{P}z(t) \\ =& \upsilon^\top(t)\Big(\mathrm{Sym}\Big\{e_1^\top \mathcal{P}e_5\Big\} + 2\lambda e_1^\top \mathcal{P}e_1\Big)\upsilon(t), \end{aligned} \tag{36}$$

$$\begin{aligned} \dot{V}_2(t) + 2\lambda V_2(t) =& \upsilon^\top(t)\Big\{\Big[(t_{k+1} - t) - (t - t_k) \\ &+ 2\lambda(t_{k+1} - t)(t - t_k)\Big]e_2^\top \mathcal{Q}e_2\Big\}\upsilon(t), \end{aligned} \tag{37}$$

$$\begin{aligned} \dot{V}_3(t) + 2\lambda V_3(t) =& -\int_{t_k}^{t} z^\top(s)ds\mathcal{T}\int_{t_k}^{t} z(s)ds \\ &+ (t_{k+1} - t)\Big[\mathrm{Sym}\Big\{\int_{z_k}^{t} z^\top(s)ds\mathcal{T}z(t)\Big\} \\ &+ 2\lambda\int_{t_k}^{t} z^\top(s)ds\mathcal{T}\int_{t_k}^{t} z(s)ds\Big] \\ =& \upsilon^\top(t)\Big[-e_3^\top \mathcal{T}e_3 + (t_{k+1} - t) \\ &\times \Big(2\lambda e_3^\top \mathcal{T}e_3 + \mathrm{Sym}\Big\{e_3^\top \mathcal{T}e_1\Big\}\Big)\Big]\upsilon(t), \end{aligned} \tag{38}$$

$$\dot{V}_4(t) + 2\lambda V_4(t) = -\eta^\top(t)\mathcal{U}\eta(t) - \gamma^\top(t)\mathcal{S}\gamma(t)$$

$$
\begin{aligned}
&+ (t_{k+1}-t)\bigg\{2\lambda\Big[\eta^\top(t)\mathcal{U}\eta(t)+\gamma^\top(t)\mathcal{S}\gamma(t)\Big] \\
&+ \mathrm{Sym}\Big\{\eta^\top(t)\mathcal{U}\dot{\eta}(t)+\gamma^\top(t)\mathcal{S}\dot{\gamma}(t)\Big\}\bigg\} \\
&= \upsilon^\top(t)\bigg\{-\rho_1^\top\mathcal{U}\rho_1-\tau_1^\top\mathcal{S}\tau_1 \\
&+ (t_{k+1}-t)\Big[2\lambda\Big(\rho_1^\top\mathcal{U}\rho_1+\tau_1^\top\mathcal{S}\tau_1\Big) \\
&+ \mathrm{Sym}\Big\{\rho_1^\top\mathcal{U}\rho_2+\tau_1^\top\mathcal{S}\tau_2\Big\}\Big]\bigg\}\upsilon(t),
\end{aligned} \tag{39}
$$

$$
\begin{aligned}
\dot{V}_5(t)+2\lambda V_5(t) &= (t_{k+1}-t)\varpi^\top(t)\mathcal{Y}\varpi(t) \\
&\quad -\int_{t_k}^{t} e^{2\lambda(s-t)}\varpi^\top(s)\mathcal{Y}\varpi(s)ds \\
&\le (t_{k+1}-t)\upsilon^\top(t)\Big(\varrho^\top\mathcal{Y}\varrho\Big)\upsilon(t) \\
&\quad - e^{-2\lambda h_M}\int_{t_k}^{t}\varpi^\top(s)\mathcal{Y}\varpi(s)ds,
\end{aligned} \tag{40}
$$

$$
\begin{aligned}
\dot{V}_6(t)+2\lambda V_6(t) &= (t_{k+1}-t)e^{-2\lambda t} \\
&\quad \times\bigg\{\int_{t_k}^{t}\frac{\partial}{\partial t}\Big[\int_{\theta}^{t}e^{2\lambda s}z^\top(s)\mathcal{X}z(s)ds\Big]d\theta\bigg\} \\
&\quad -\int_{t_k}^{t}\int_{\theta}^{t}e^{2\lambda(s-t)}z^\top(s)\mathcal{X}z(s)dsd\theta \\
&\le (t_{k+1}-t)(t-t_k)\upsilon^\top(t)\Big(e_1^\top\mathcal{X}e_1\Big)\upsilon(t) \\
&\quad - e^{-2\lambda h_M}\int_{t_k}^{t}\int_{\theta}^{t}z^\top(s)\mathcal{X}z(s)dsd\theta.
\end{aligned} \tag{41}
$$

When calculating $\dot{V}(t)+2\lambda V(t)$, some integral terms and sampling instant coupled terms are produced. Nextly, in the steps (i)-(iii), these terms are properly treated to formulate the numerically tractable result.

(i) From the complete square formula with $t_{k+1}-t_k\le h_M$, it is obtained that

$$
(t_{k+1}-t)(t-t_k)\le\frac{1}{4}\big[(t_{k+1}-t)+(t-t_k)\big]h_M. \tag{42}
$$

Therefore, in retrospect of (37), due to $\mathcal{Q}>0$, $\dot{V}_2(t)+2\lambda V_2(t)$ can be estimated as

$$
\begin{aligned}
\dot{V}_2(t)+2\lambda V_2(t) &\le \upsilon^\top(t)\bigg\{\Big[\Big(\frac{1}{2}\lambda h_M-1\Big)(t-t_k) \\
&\quad +\Big(\frac{1}{2}\lambda h_M+1\Big)(t_{k+1}-t)\Big]e_2^\top\mathcal{Q}e_2\bigg\}\upsilon(t).
\end{aligned} \tag{43}
$$

(ii) Revisiting (40), the following equation can be confirmed by calculation:

$$
\begin{aligned}
-\int_{t_k}^{t}\varpi^\top(s)\mathcal{Y}\varpi(s)ds &= -\upsilon^\top(t)\Big[(t-t_k)e_2^\top\mathcal{Y}_{22}e_2 \\
&\quad +\mathrm{Sym}\{e_3^\top\mathcal{Y}_{12}e_2\}\Big]\upsilon(t)-\int_{t_k}^{t}z^\top(s)\mathcal{Y}_{11}z(s)ds.
\end{aligned} \tag{44}
$$

In view of the Wirtinger-based integral inequality (24) with $\mathcal{Y}_{11}>0$, it can be deduced that

$$
-\int_{t_k}^{t}z^\top(s)\mathcal{Y}_{11}z(s)ds\le-\upsilon^\top(t)\Bigg(\frac{\iota_1^\top\mathcal{Y}_{11}\iota_1+3\iota_2^\top\mathcal{Y}_{11}\iota_2}{t-t_k}\Bigg)\upsilon(t). \tag{45}
$$

For any matrices $\mathcal{H}_i$ $(i=1,2)$, it is obviously found that $\frac{1}{t-t_k}\left[\mathcal{Y}_{11}\iota_i-(t-t_k)\mathcal{H}_i\right]^\top\mathcal{Y}_{11}^{-1}\left[\mathcal{Y}_{11}\iota_i-(t-t_k)\mathcal{H}_i\right]\ge 0$, which is equivalent to

$$
-\frac{1}{t-t_k}\iota_i^\top\mathcal{Y}_{11}\iota_i\le(t-t_k)\mathcal{H}_i^\top\mathcal{Y}_{11}^{-1}\mathcal{H}_i-\mathrm{Sym}\Big\{\iota_i^\top\mathcal{H}_i\Big\}. \tag{46}
$$

Injecting (44)-(46) into (40), one can acquire that

$$
\begin{aligned}
&\dot{V}_5(t)+2\lambda V_5(t)\le\upsilon^\top(t)\bigg\{(t_{k+1}-t)\varrho^\top\mathcal{Y}\varrho+e^{-2\lambda h_M} \\
&\times\Big\{-(t-t_k)e_2^\top\mathcal{Y}_{22}e_2-\mathrm{Sym}\Big\{e_3^\top\mathcal{Y}_{12}e_2\Big\}+\sum_{i=1}^{2}(2i-1) \\
&\times\Big[(t-t_k)\mathcal{H}_i^\top\mathcal{Y}_{11}^{-1}\mathcal{H}_i-\mathrm{Sym}\Big\{\iota_i^\top\mathcal{H}_i\Big\}\Big]\Big\}\bigg\}\upsilon(t).
\end{aligned} \tag{47}
$$

(iii) By means of double integral type of Jensen inequality (25), it is direct to reach

$$
-\int_{t_k}^{t}\int_{\theta}^{t}z^\top(s)\mathcal{X}z(s)dsd\theta\le-2\upsilon^\top(t)\Big(e_4^\top\mathcal{X}e_4\Big)\upsilon(t). \tag{48}
$$

Furthermore, from (42), it can be found that

$$
\begin{aligned}
&(t_{k+1}-t)(t-t_k)\upsilon^\top(t)\Big(e_1^\top\mathcal{X}e_1\Big)\upsilon(t) \\
&\le\frac{1}{4}h_M\big[(t_{k+1}-t)+(t-t_k)\big]\upsilon^\top(t)\Big(e_1^\top\mathcal{X}e_1\Big)\upsilon(t).
\end{aligned} \tag{49}
$$

Considering (41), it is inferred from (48) and (49) that

$$
\begin{aligned}
\dot{V}_6(t)+2\lambda V_6(t) &\le\upsilon^\top(t)\bigg\{\frac{1}{4}h_M\big[(t_{k+1}-t) \\
&\quad +(t-t_k)\big]e_1^\top\mathcal{X}e_1-2e^{-2\lambda h_M}e_4^\top\mathcal{X}e_4\bigg\}\upsilon(t).
\end{aligned} \tag{50}
$$

So far, the upper bound for $\dot{V}(t)+2\lambda V(t)$ is suitably expressed in terms of linear form with regard to $\upsilon(t)$. Then, for any scalars ψ_1, ψ_2, and any matrix $\mathcal{L}$ of proper size, it is inferred from (22) that

$$
\begin{aligned}
0 &= 2\Big[z^\top(t)\mathcal{L}+\psi_1 z^\top(t_k)\mathcal{L}+\psi_2\dot{z}^\top(t)\mathcal{L}\Big]\bigg\{-\dot{z}(t) \\
&\quad +\sum_{j=1}^{\kappa}\mathscr{D}_j(\xi(z_1(t_k)))\big[\mathcal{A}z(t)+\mathcal{C}_j\mathcal{G}_j\mathcal{E}z(t_k)+\mathcal{D}\phi(t)\big]\bigg\}.
\end{aligned} \tag{51}
$$

Moreover, introducing an additional positive scalar variable γ, it follows from (3) that

$$
\sigma^2\gamma-\phi^\top(t)\gamma\phi(t)\ge 0. \tag{52}
$$

Denoting $\mathcal{K}_j = \mathcal{L}\mathcal{C}_j\mathcal{G}_j$ and $\bar{\upsilon}(t) = \mathrm{col}\{\upsilon(t),\ \phi(t)\}$, for $t \in [t_k, t_{k+1})$, taking into account (36)-(52) results in

$$\begin{aligned}\dot{V}(t) + 2\lambda V(t) \le& \sum_{m=1}^{6}\Big[\dot{V}_m(t) + 2\lambda V_m(t)\Big] - \phi^\top(t)\gamma\phi(t)\\ &+ \sigma^2\gamma \le \sigma^2\gamma + \sum_{j=1}^{\kappa}\mathscr{D}_j(\xi(z_1(t_k)))\bar{\upsilon}^\top(t)\Bigg\{\frac{t_{k+1}-t}{h_k}\\ &\times\Big(\varLambda_j + h_k\varPi\Big) + \frac{t-t_k}{h_k}\Big\{\varLambda_j + h_k\Big(\varGamma + \varDelta\Big)\Big\}\Bigg\}\bar{\upsilon}(t),\end{aligned} \tag{53}$$

where $\varDelta = \mathrm{diag}\Big\{e^{-2\lambda h_M}\sum_{i=1}^{2}(2i-1)\mathcal{H}_i^\top\mathcal{Y}_{11}^{-1}\mathcal{H}_i,\ \ \mathbf{0}\Big\}$.

Resorting to the Schur complement once again, $\varOmega_{2j}(h_k) < 0$ is equivalent to

$$\varLambda_j + h_k\Big(\varGamma + \varDelta\Big) < 0. \tag{54}$$

Besides, $\varOmega_{ij}(h_k)$ $(i = 1, 2)$ can be described as the convex combination forms:

$$\varOmega_{ij}(h_k) = \frac{h_M - h_k}{h_M - h_m}\varOmega_{ij}(h_m) + \frac{h_k - h_m}{h_M - h_m}\varOmega_{ij}(h_M). \tag{55}$$

As fuzzy membership functions $\mathscr{D}_j(\xi(t_k))$ are of intrinsically nonnegative property, if the inequalities (27) and (28) are feasible at the vertices of $h_k \in [h_m, h_M]$, it is indicated that

$$\dot{V}(t) + 2\lambda V(t) \le \sigma^2\gamma. \tag{56}$$

Pre-multiplying and post-multiplying both sides of (56) by $e^{2\lambda t}$, respectively, it gives rise to $\Big[e^{2\lambda t}V(t)\Big]' \le \sigma^2 e^{2\lambda t}\gamma$. Then, performing integral operation from t_k to t yields

$$V(t) \le e^{-2\lambda(t-t_k)}V(t_k) + \sigma^2\int_{t_k}^{t} e^{-2\lambda(t-s)}\gamma ds. \tag{57}$$

Bearing in mind $\lim_{t\to t_k^-}V(t) = V(t_k)$, it holds that

$$\begin{aligned}V(t) \le& e^{-2\lambda(t-t_k)}V(t_k^-) + \sigma^2\int_{t_k}^{t} e^{-2\lambda(t-s)}\gamma ds\\ \le& e^{-2\lambda(t-t_{k-1})}V(t_{k-1}^-) + \sigma^2\int_{t_k}^{t} e^{-2\lambda(t-s)}\gamma ds\\ &+ \sigma^2 e^{-2\lambda(t-t_k)}\int_{t_{k-1}}^{t_k} e^{-2\lambda(t_k-s)}\gamma ds \le \cdots\\ \le& \sum_{l=1}^{k}\Big[\sigma^2 e^{-2\lambda(t-t_l)}\int_{t_{l-1}}^{t_l} e^{-2\lambda(t_l-s)}\gamma ds\Big]\\ &+ \sigma^2\int_{t_k}^{t} e^{-2\lambda(t-s)}\gamma ds + e^{-2\lambda t}V(0).\end{aligned} \tag{58}$$

Summing up the integral terms at the right hand side of (58), one can acquire that

$$V(t) \le e^{-2\lambda t}V(0) + \frac{1}{2\lambda}\Big(1 - e^{-2\lambda t}\Big)\sigma^2\gamma. \tag{59}$$

From the formation of STDLF (31), due to $V_n(0) = 0$ $(n = 2, \cdots, 6)$, it is found that $V(0) = V_1(0) = z^\top(0)\mathcal{P}z(0)$. Then, since $0 < 1 - e^{-2\lambda t} < 1$, by (59), it is deduced that

$$\rho_{\min}(\mathcal{P})\|z(t)\|^2 \le e^{-2\lambda t}V_1(0) + \frac{1}{2\lambda}\sigma^2\gamma, \tag{60}$$

which implies that

$$\begin{aligned}\|z(t)\| \le& \sqrt{\frac{V_1(0)}{\rho_{\min}(\mathcal{P})}}e^{-\lambda t} + \frac{\sigma}{\sqrt{2\lambda}}\sqrt{\frac{\gamma}{\rho_{\min}(\mathcal{P})}}\\ \le& \sqrt{\frac{\rho_{\max}(\mathcal{P})}{\rho_{\min}(\mathcal{P})}}\|z(0)\|e^{-\lambda t} + \frac{\sigma}{\sqrt{2\lambda}}\sqrt{\frac{\gamma}{\rho_{\min}(\mathcal{P})}}.\end{aligned} \tag{61}$$

As a consequence, the estimation error dynamics (22) with aperiodic sampling is exponentially ultimately bounded with decay rate λ and decay coefficient $\sqrt{\frac{\rho_{\max}(\mathcal{P})}{\rho_{\min}(\mathcal{P})}}$. As $t \to +\infty$, the observation error $z(t)$ is guaranteed to satisfy

$$\lim_{t\to+\infty}\|z(t)\| = \frac{\sigma}{\sqrt{2\lambda}}\sqrt{\frac{\gamma}{\rho_{\min}(\mathcal{P})}}. \tag{62}$$

From (16), it is known that $\mathcal{C}_j$ are invertible, and thus the observer gain matrices are given as $\mathcal{G}_j = \mathcal{C}_j^{-1}\mathcal{L}^{-1}\mathcal{K}_j$. In this way, the proof is completed.

Remark 6: In the Theorem 1, in view of aperiodic sampling, the sufficient condition is presented to guarantee the exponential convergence for the estimation error dynamics between the TSFESO and uncertain nonlinear systems. For analysis of sampled-data systems, it is a prerequisite to select a positive definite Lyapunov function. In the existing literatures [4, 7, 9], much attention is attracted to ensure positivity of each Lyapunov term. In virtue of elaborate construction of sampling- and time-dependent terms multiplied by proper augmented vectors, it is noticed that $V_i(t)|_{t=t_k} = V_i(t)|_{t=t_{k+1}}$ $(i = 3, 4)$, and thus the looped function requirement is satisfied, which significantly enlarges the feasible space.

Remark 7: The conspicuous features of newly established STDLF (31) lie in three aspects: 1) The integral term $\int_{t_k}^{t} z(s)ds$ is involved in the augmented vectors $\eta(t)$ and $\gamma(t)$, and the integrals for the quadratics are given in $V_4(t)$ and $V_5(t)$. 2) Taking advantages of sampling- and time-dependent terms coupled with $V_2(t)$-$V_6(t)$, a great many of cross terms emerge when differentiating $V(t)$, and thus extensive relationships among system state, sampled state, single and double integrals are fundamentally consolidated by matrix variables. 3) The convergence criterion is presented as convex combinations for h_k-related inequalities, which takes the lower and upper bounds for sampling interval into account. As a result, the characteristics of sampling behavior are sufficiently reflected. From the viewpoints of Lyapunov function construction, it can be predicted that the Theorem 1 will yield more preferable performance.

V. Numerical Examples

In this section, an illustrative numerical example is given to verify the advantages and effectiveness of the TSFESO design approach.

Example 1: Consider a second-order system based on the example borrowed from [28]

$$\begin{cases}\dot{x}_1(t) = x_2(t)\\ \dot{x}_2(t) = f(t, x_1(t), x_2(t)) + w(t) + u(t)\\ y(t) = x_1(t),\end{cases} \tag{63}$$

where the unmodeled dynamics is described by $f(t,x_1,x_2)= -3x_1-2x_2-\sin^3(x_1+x_2)$, and the external disturbance is given as

$$w(t)=\begin{cases}0, & t<4\pi \text{ or } t>6\pi\\ -0.4\cos(2t)+0.4, & 4\pi\le t\le 6\pi.\end{cases} \tag{64}$$

The control input is selected as $u=2x_1+x_2$. From (2), the extended state representing total disturbance is expressed by $x_3=w-3x_1-2x_2-\sin^3(x_1+x_2)$.

For comparison purpose, the performance for the LESO, ε-dependent NESO, and the proposed TSFESO are presented under a mismatched initial estimated value.

(i) Taking into account of non-sampled observation and introducing positive observer gains l_1, l_2, and l_3, the LESO can be constructed as

$$\begin{cases}\dot{\hat{x}}_1(t)=\hat{x}_2(t)-l_1z_1(t)\\ \dot{\hat{x}}_2(t)=\hat{x}_3(t)-l_2z_1(t)+u(t)\\ \dot{\hat{x}}_3(t)=-l_3z_1(t).\end{cases} \tag{65}$$

The characteristic polynomial for the system matrix of the error equation is $\lambda(s)=s^3+l_1s^2+l_2s+l_3$. It is obvious that if the roots for $\lambda(s)$ are all in the left half plane and ϕ is bounded, the LESO is bounded-input-bounded-output. For simplicity, assign $\lambda(s)=(s+\omega_o)^3$, and then one can compute that $l_1=3\omega_o$, $l_2=3\omega_o^2$, and $l_3=\omega_o^3$, where ω_o is the observer bandwidth [29].

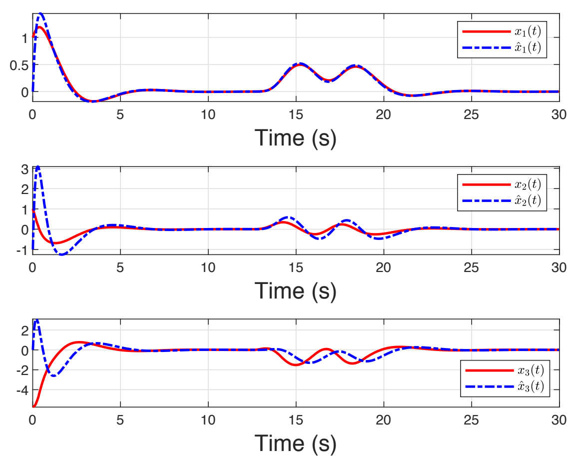

Fig. 1: Estimation performance of LESO ($\omega_0=5$).

(ii) Considering the continuous data transmission mechanism, the ε-dependent NESO as in [29] is designed as follows:

$$\begin{cases}\dot{\hat{x}}_1(t)=\hat{x}_2(t)+\dfrac{3}{\varepsilon}\Big[-z_1(t)\Big]+\varepsilon\varphi\Big[-\dfrac{1}{\varepsilon^2}z_1(t)\Big]\\ \dot{\hat{x}}_2(t)=\hat{x}_3(t)+\dfrac{3}{\varepsilon^2}\Big[-z_1(t)\Big]+u(t)\\ \dot{\hat{x}}_3(t)=\dfrac{1}{\varepsilon^3}\Big[-z_1(t)\Big],\end{cases} \tag{66}$$

where

$$\varphi(\theta)=\begin{cases}\dfrac{1}{4}\text{sign}(\theta), & |\theta|>\dfrac{1}{2}\pi\\ \dfrac{1}{4}\sin\theta, & |\theta|\le\dfrac{1}{2}\pi.\end{cases} \tag{67}$$

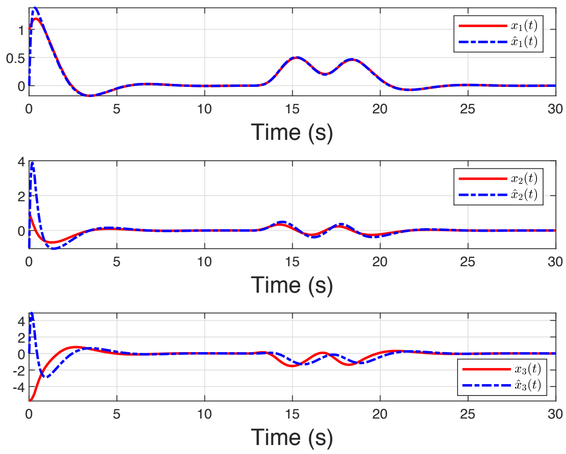

Fig. 2: Estimation performance of NESO ($\varepsilon=0.3$).

(iii) For fair comparison, a general TSFESO is established by use of the identical arithmetic units as in (66), namely $\vartheta_1(\theta)=3\theta+\varphi(\theta)$, $\vartheta_2(\theta)=3\theta$, and $\vartheta_3(\theta)=\theta$. Moreover, by simple calculation, one has

$$\begin{aligned}|\phi|=|\dot f+\dot w|&\le\left|\frac{\partial f}{\partial x_1}\dot x_1\right|+\left|\frac{\partial f}{\partial x_2}\dot x_2\right|+|\dot w|\\ &\le 5|x_1|+11|x_2|+9.8.\end{aligned} \tag{68}$$

According to [37], from the expression of the disturbance w, the solution of (63) is bounded, and then the *Assumption* (H1) is satisfied with boundedness for $|\phi|$.

Based on (13) assuming $|z_1(t_k)|\le 6$, the sampled-data fuzzy membership functions for $\vartheta_1(z_1(t_k))$ are described by

$$\begin{cases}\mathscr{L}_{11}(\xi_1(t_k))=\dfrac{\frac{13}{4}z_1(t_k)-\vartheta_1(z_1(t_k))}{\frac{5}{24}z_1(t_k)}\\ \mathscr{L}_{12}(\xi_1(t_k))=\dfrac{\vartheta_1(z_1(t_k))-\frac{73}{24}z_1(t_k)}{\frac{5}{24}z_1(t_k)}.\end{cases} \tag{69}$$

Due to linearity of $\vartheta_2(\cdot)$ and $\vartheta_3(\cdot)$, by T-S fuzzy modeling procedure (20), a sampled-data TSFESO composed of two fuzzy rules can be felicitously formulated in form of (21) with $n=2$. The normalized membership functions and system matrices are given as

$$\mathscr{D}_1(\xi(t_k))=\mathscr{L}_{11}(\xi_1(t_k)),\ \mathscr{D}_2(\xi(t_k))=\mathscr{L}_{12}(\xi_1(t_k))$$

$$\mathcal{A}=\begin{bmatrix}0&1&0\\0&0&1\\0&0&0\end{bmatrix},\ \mathcal{B}=\begin{bmatrix}0\\1\\0\end{bmatrix},\ \mathcal{G}_j=\begin{bmatrix}-\eta_{j1}\\-\eta_{j2}\\-\eta_{j3}\end{bmatrix}$$

$$\mathcal{C}_1=\text{diag}\left\{\frac{73}{24},\ 3,\ 1\right\},\ \mathcal{C}_2=\text{diag}\left\{\frac{13}{4},\ 3,\ 1\right\}.$$

Choosing the sampling interval parameters $h_m=1$ms and $h_M=3$ms, by the use of the Theorem 1 with $\psi_1=1$, $\psi_2=0.015$, and $\lambda=0.05$, one can attain an admissible TSFESO with the observer gain matrices

$$\mathcal{G}_1=\begin{bmatrix}-41.9640 & -241.2850 & -1315.3146\end{bmatrix}^\top,$$
$$\mathcal{G}_2=\begin{bmatrix}-52.1708 & -242.5952 & -1315.9713\end{bmatrix}^\top.$$

Assuming the initial conditions $x(0) = [1, 1]^\top$ and $\hat{x}(0) = [0, -1, 0]^\top$, the state estimation performances for LESO (65) with $\omega_0 = 5$ and NESO (66) with $\varepsilon = 0.3$ under continuous data transmission are presented in the Fig. 1 and Fig. 2. Considering the aperiodic sampling situation 1ms$\leq h_k \leq$3ms, the state response for the proposed TSFESO with $\mathcal{G}_1$ and $\mathcal{G}_2$ is depicted in the Fig. 3. The corresponding estimation errors are shown in the Fig. 4-6, respectively. From Fig. 4, it is noticeable that the assumption $|z_1(t_k)| \leq 6$ is satisfied, and thus the prerequisite for application of TSFESO holds.

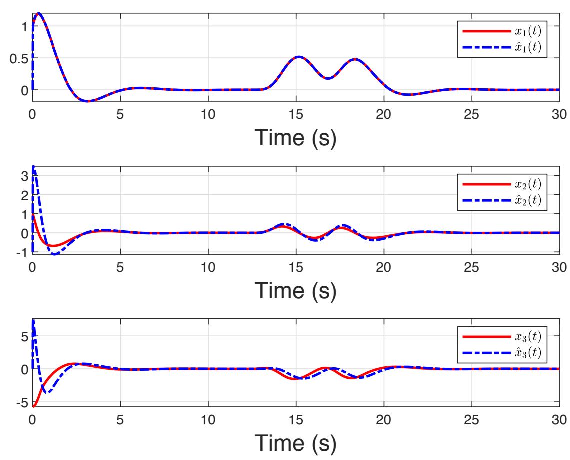

Fig. 3: Estimation performance of TSFESO.

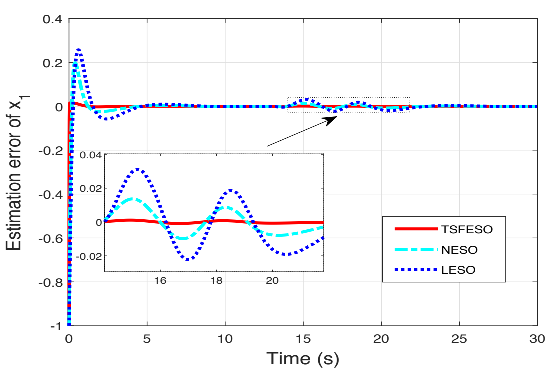

Fig. 4: Estimation error comparison for $x_1(t)$.

As seen from the Fig. 3, it is illustrated that both of the system states and total disturbance are tracked satisfactorily by TSFESO. Combining Figs. 1-3 and Fig. 4, in contrast to LESO and NESO, the convergence time of TSFESO for output $y(t) = x_1(t)$ is significantly shorter with a very small peaking value of estimation error. By the Figs. 5-6, for the system state involving uncertainty $x_2(t)$ and the extended state $x_3(t)$, the observation performance of TSFESO is obviously preferable than LESO, and comparative with NESO, even though the observer input is sampled aperiodically.

As shown in Figs. 4-6, the estimation errors for stead-state behaviors of TSFESO converge to a sufficiently small region $\mathcal{E}[z_i(t)]$ satisfying $|z_i(t)| \leq \mathcal{E}[z_i(t)]$ $(i = 1, 2, 3)$. In the Table I, the convergence regions of LESO, NESO, and TSFESO are listed. In order to verify the advantages of TSFESO, the percentage of improvement of TSFESO over LESO (PITOL) and NESO (PITON) on convergence regions are introduced, which are defined as follows:

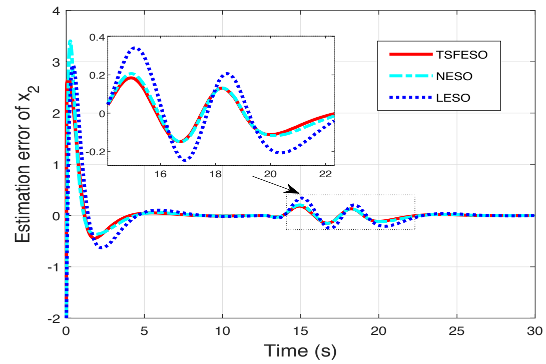

Fig. 5: Estimation error comparison for $x_2(t)$.

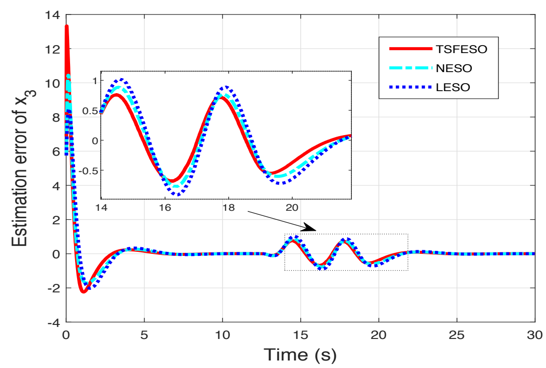

Fig. 6: Estimation error comparison for $x_3(t)$.

$$\text{PITOL(PITON)} = \frac{|\mathcal{E}[z_i(t)]_{\text{TSFESO}} - \mathcal{E}[z_i(t)]_{\text{LESO(NESO)}}|}{\mathcal{E}[z_i(t)]_{\text{LESO(NESO)}}} \times 100\%.$$

From Table I, it is distinctly discovered that the TSFESO achieves desirable ultimate boundedness, and produces significant superiority over LESO and NESO on stead-state behaviors.

TABLE I: Convergence regions for estimation errors of LESO, NESO, and TSFESO

Convergence regions	$\mathcal{E}[z_1(t)]$	$\mathcal{E}[z_2(t)]$	$\mathcal{E}[z_3(t)]$
LESO ($\omega_o = 5$)	2.3199×10^{-4}	3.4198×10^{-3}	1.5449×10^{-2}
NESO ($\varepsilon = 0.3$)	5.5335×10^{-6}	1.1928×10^{-4}	4.6550×10^{-4}
TSFESO	4.9143×10^{-7}	8.6196×10^{-5}	3.9296×10^{-4}
PITOL	99.79%	96.50%	97.79%
PITON	91.12%	27.74%	15.58%

Compared with the LESO (65), the strengths of nonlinear estimation of TSFESO are incisively revealed for both of response time and observation capacity, which benefit from the nonlinear property produced by fuzzy membership functions. Different from the NESO of ε-related observer gains (66), the fuzzy-dependent observer gains $\mathcal{G}_j$ are introduced in TSFESO to give additional degree of freedom. Moreover, the strict stability proof is conveniently achieved by light of T-S fuzzy formulation, and meanwhile, the aperiodic sampled-data is expediently compatible. By virtue of local characteristic for TSFESO, the STDLF and improved integral inequalities are applicable such that some extra feasible space is relaxed to produce performance promotion. It is noticeable that $\vartheta_2(\theta)$ and $\vartheta_3(\theta)$ are chosen as linear functions. In order to exploit better observation efficiency in more practical scenarios, one can readily inject nonlinear functions into (21) with various constraint factors by elaborate architecture of TSFESO. However, such a treatment may be infeasible in context of NESO, since some unpredictable difficulties are inevitably encountered in the deriving process. As a consequence, the preferable nonlinear estimating efficiency and desirable linear numerical tractability are integrated in a unified framework of TSFESO with potential for performance improvement.

VI. Conclusion

In this paper, based on sampled-data transmission mechanism, the ESO design is investigated for a class of uncertain nonlinear systems. In order to balance efficient observation operation and strict stability accessibility, a novel methodology of TSFESO with fuzzy-dependent observer gains is put forward for the first time. By means of fuzzy membership functions, the estimating action is globally implemented in nonlinear pattern, while taking advantages of T-S fuzzy formation, the observer gains are locally calculated in linear manner. Therefore, the proposed TSFESO can be recognized as a collective architecture for nonlinear estimating efficiency and linear numerical tractability. By constructing a STDLF, the exponential convergence criterion along with observer design approach is presented for TSFESO subject to aperiodic sampling, in which the relationships among fuzzy membership-related parameters, variable sampling interval, decay rate, decay coefficient, and estimated bound are quantitatively reflected. An illustrative example is presented to demonstrate the superiorities and effectiveness of the proposed approach.

The future work will focus on two mainstream lines: the one is to extend the TSFESO to uncertain nonlinear systems with networked phenomena, such as event-triggered strategy, cyber attacks, and communication protocol; the other one is to apply the TSFESO to control synthesis and fault detection or develop the corresponding T-S fuzzy ADRC scheme.

References

[1] Y. M. Li and S. C. Tong, "Adaptive fuzzy control with prescribed performance for block-triangular-structured nonlinear systems," *IEEE Trans. Fuzzy Syst.*, vol. 26, no. 3, pp. 1153-1163, Jun. 2018.
[2] X. Wang, J. H. Park, K. She, S. M. Zhong, and L. Shi, "Stabilization of chaotic systems with T-S fuzzy model and nonuniform sampling: a switched fuzzy control approach," *IEEE Trans. Fuzzy Syst.*, vol. 27, no. 6, pp. 1263-1271, Jun. 2019.
[3] Z. X. Zhang, H. J. Liang, C. W. Wu, and C. K. Ahn, "Adaptive event-triggered output feedback fuzzy control for nonlinear networked systems with packet dropouts and actuator failure ," *IEEE Trans. Fuzzy Syst.*, vol. 27, no. 9, pp. 1793-1806, Sep. 2019.
[4] H. Y. Li, Y. N. Pan, P. Shi, and Y. Shi, "Switched fuzzy output feedback control and its application to a mass-spring-damping system," *IEEE Trans. Fuzzy Syst.*, vol. 24, no. 6, pp. 1259-1269, Dec. 2016.
[5] A. Q. Wang, L. Liu, J. B. Qiu, and G. Feng, "Event-triggered robust adaptive fuzzy control for a class of nonlinear systems," *IEEE Trans. Fuzzy Syst.*, vol. 27, no. 8, pp. 1648-1658, Aug. 2019.
[6] L. Liu, Y.-J. Liu, and S. C. Tong, "Fuzzy-based multierror constraint control for switched nonlinear systems and its applications," *IEEE Trans. Fuzzy Syst.*, vol. 27, no. 8, pp. 1519-1531, Aug. 2019.
[7] B. Cai, L. X. Zhang, and Y. Shi, "Control synthesis of hidden semi-Markov uncertain fuzzy systems via observations of hidden modes ," *IEEE Trans. Fuzzy Syst.*, vol. 50, no. 8, pp. 3709-3718, Aug. 2020.
[8] T. S. Tong, K. K. Sun, and S. Sui, "Observer-based adaptive fuzzy decentralized optimal control design for strict-feedback nonlinear large-scale systems," *IEEE Trans. Fuzzy Syst.*, vol. 26, no. 2, pp. 569-584, Apr. 2018.
[9] X. D. Zhao, Y. F. Yin, B. Niu, and X. L. Zheng, "Stabilization for a class of switched nonlinear systems with novel average dwell time switching by T-S fuzzy modeling," *IEEE Trans. Cybern.*, vol. 46, no. 8, pp. 1952-1957, Aug. 2016.
[10] X. J. Su, F. Q. Xia, Y.-D. Song, M. V. Basin, and L. Zhao, "$\mathcal{L}_2-\mathcal{L}_\infty$ output feedback controller design for fuzzy systems over switching parameters," *IEEE Trans. Cybern.*, vol. 26, no. 6, pp. 3755-3769, Dec. 2018.
[11] L. K. Wang and H.K. Lam, "A new approach to stability and stabilization analysis for continuous-time Takagi-Sugeno fuzzy systems with time delay," *IEEE Trans. Fuzzy Syst.*, vol. 26, no. 4, pp. 2460-2465, Aug. 2018.
[12] Z. Lian, Y. He, C.-K. Zhang, P. Shi, and M. Wu, "Robust H_∞ control for T-S fuzzy systems with state and input time-varying delays via delay-product-type functional method," *IEEE Trans. Cybern.*, vol. 27, no. 10, pp. 1917-1930, Oct. 2019.
[13] H. Shen, M. S. Chen, Z.-G. Wu, J. D. Cao, and J. H. Park, "Reliable event-triggered asynchronous extended passive control for semi-Markov jump fuzzy systems and its application," *IEEE Trans. Fuzzy Syst.*, vol. 28, no. 8, pp. 1708-1722, Aug. 2020.
[14] X.-M. Zhang, Q.-L. Han, and X. H. Ge, "A novel finite-sum inequality-based method for robust H_∞ control of uncertain discrete-time Takagi-Sugeno fuzzy systems with interval-like time-varying delays," *IEEE Trans. Cybern.*, vol. 48, no. 9, pp. 2569-2582, Sep. 2018.
[15] C. Z. Zhang, H.K. Lam, J. B. Qiu, C. J. Liu, and Q. J. Chen, "A new design of membership-function-dependent controller for T-S fuzzy systems under imperfect premise matching," *IEEE Trans. Fuzzy Syst.*, vol. 27, no. 7, pp. 1428-1440, Jul. 2019.
[16] X. X. Liu, X. J. Su, P. Shi, and C. Shen, "Observer-based sliding mode control for uncertain fuzzy systems via event-triggered strategy," *IEEE Trans. Fuzzy Syst.*, vol. 27, no. 11, pp. 2190-2201, Nov. 2019.
[17] D. Zhang, H. Y. Song, and L. Yu, "Robust fuzzy-model-based filtering for nonlinear cyber-physical systems with multiple stochastic incomplete measurements ," *IEEE Trans. Syst., Man, Cybern., Syst.*, vol. 47, no. 8, pp. 1826-1838, Aug. 2017.
[18] J. Q. Han, "From PID to active disturbance rejection control," *IEEE Trans. Ind. Electron.*, vol. 56, no. 3, pp. 900-906, Mar. 2009.
[19] B.-Z. Guo and F.-F. Jin, "The active disturbance rejection and sliding mode control approach to the stabilization of the Euler-Bernoulli beam equation with boundary input disturbance," *Automatica*, vol. 49, no. 9, pp. 2911-2918, Sep. 2013.
[20] F. Liu, Y. Li, Y. Cao, J.-H. She, and M. Wu, "A two-layer active disturbance rejection controller design for load frequency control of interconnected power system," *IEEE Trans. Power Syst.*, vol. 31, no. 4, pp. 3320-3321, Jul. 2016.
[21] Y. Q. Xia, M. Y. Fu, C. M. Li, F. Pu, and Y. W. Xu, "Active disturbance rejection control for active suspension system of tracked vehicles with gun," *IEEE Trans. Ind. Electron.*, vol. 65, no. 5, pp. 4051-4060, May. 2018.
[22] X. C. Xue, W. Y. Bai, S. Yang, K. Song, Y. Huang, and H. Xie, "ADRC with adaptive extended state observer and its application to air-fuel ratio control in gasoline engines," *IEEE Trans. Ind. Electron.*, vol. 62, no. 9, pp. 5847-5857, Sep. 2015.
[23] C. Ren, X. H. Li, X. B. Yang, and S. G. Ma, "Extended state observer-based sliding mode control of an omnidirectional mobile robot with friction compensation," *IEEE Trans. Ind. Electron.*, vol. 66, no. 12, pp. 9480-9489, Dec. 2019.
[24] R. J. Dian, W. Xu, J. G. Zhu, D. Hu, and Y. Liu, "An improved speed sensorless control strategy for linear induction machines based on extended state observer for linear metro drives," *IEEE Trans. Vel. Technol.*, vol. 67, no. 10, pp. 9198-9210, Oct. 2018.
[25] B.-Z. Guo and Z.-L. Zhao, "On the convergence of an extended state observer for nonlinear systems with uncertainty," *Syst. Control Lett.*, vol. 60, no. 6, pp. 420-430, Jun. 2011.
[26] M. P. Ran, Q. Wang, and C. Y. Dong, "Stabilization of a class of nonlinear systems with actuator saturation via active disturbance rejection control," *Automatica*, vol. 63, pp. 302-310, Jan. 2016.

[27] B.-Z. Guo and Z.-L. Wu, "Output tracking for a class of nonlinear systems with mismatched uncertainties by active disturbance rejection control," *Syst. Control Lett.*, vol. 100, pp. 21-31, Feb. 2017.
[28] Y. Huang, J. Z. Wang, D. W. Shi, and L. Shi, "Toward event-triggered extended state observer," *IEEE Trans. Autom. Control*, vol. 63, no. 6, pp. 1842-1849, Jun. 2018.
[29] D. Yoo, S. Yau, and Z. Q. Gao, "Optimal fast tracking observer bandwidth of the linear extended state observer," *Int. J. Control*, vol. 80, no. 1, pp. 102-111, Jan. 2007.
[30] W. Tan and C. F. Fu, "Linear active disturbance-rejection control: analysis and tuning via IMC," *IEEE Trans. Ind. Electron.*, vol. 63, no. 4, pp. 2350-2359, Apr. 2016.
[31] J. K. Sun, J. Yang, S. H. Li, and W. X. Zheng, "Sampled-data-based event-triggered active disturbance rejection control for disturbed systems in network environment," *IEEE Trans. Cybern.*, vol. 49, no. 2, pp. 556-566, Feb. 2019.
[32] Y. Huang, J. Z. Wang, D. W. Shi, J. F. Wu, and L. Shi, "Event-triggered sampled-data control: an active disturbance rejection approach," *IEEE/ASME Trans. Mechatron.*, vol. 24, no. 5, pp. 2052-2063, Oct. 2019.
[33] Y. Yuan, Y. Yu, Z. Wang, and L. Guo, "A sampled-data approach to nonlinear ESO-based active disturbance rejection control for pneumatic muscle actuator systems with actuator saturations," *IEEE Trans. Ind. Electron.*, vol. 66, no. 6, pp. 4608-4617, Jun. 2019.
[34] A. Seuret and F. Gouaisbaut, "Wirtinger-based integral inequality: Application to time-delay systems," *Automatica*, vol. 49, no. 9, pp. 2860-2866, Sep. 2013.
[35] J. Sun, G. P. Liu, J. Chen, and D. Rees, "Improved delay-range-dependent stability criteria for linear systems with time-varying delays," *Automatica*, vol. 46, no. 2, pp. 466-470, Feb. 2010.
[36] A. Seuret, "A novel stability analysis of linear systems under asynchronous sampling," *Automatica*, vol. 48, no. 1, pp. 177-182, Jan. 2012.
[37] H. K. Khalil, *Nonlinear Systems*. Englewood Cliffs, NJ, USA: Prentice-Hall, 2002.